View Article Online / Journal Homepage / Table of Contents for this issue
Dynamic Article Links

Dalton Transactions

Cite this: *Dalton Trans.*, 2012, **41**, 13795

www.rsc.org/dalton

COMMUNICATION

Selective growth of Au nanograins on specific positions (tips, edges and facets) of Cu_2O octahedrons to form Cu_2O–Au hierarchical heterostructures†

Han Zhu,[a] MingLiang Du,*[a,b] DongLiang Yu,[a] Yin Wang,[c] MeiLing Zou,[a] CongSheng Xu[a] and YaQin Fu[a,b]

Received 6th July 2012, Accepted 30th July 2012
DOI: 10.1039/c2dt31487h

Published on 01 August 2012 on http://pubs.rsc.org | doi:10.1039/C2DT31487H
Downloaded by Zhejiang Sci Tech University on 24 November 2012

This communication demonstrates a novel strategy for the selective growth of Au nanograins (AuNGs) on specific positions (tips, edges and facets) of Cu_2O octahedrons to form Cu_2O–Au hierarchical heterostructures. The surface energy distribution of the octahedrons generally follows the order of $\gamma_{(facets)} < \gamma_{(edges)} < \gamma_{(tips)}$ and leads to the preferential growth and evolution of the heterostructures. These novel Cu_2O–Au hierarchical heterostructures show fascinating degradations of methylene blue (MB), due to the suppressed electron/hole recombination phenomena and the highly efficient light harvesting.

The rational growth of heterostructure nanocrystals with multiple components and tailored geometries is of significant interest because of their multifunctional properties and new features arising from the effective coupling of their different domains.[1,2] The attraction of multicomponent nanostructures is that multiple functions can be incorporated into one system for specific applications and for fascinating new properties induced by the hetero-interfaces.[3,4] In such systems, each component usually retains its original properties while modifications are confined to the interfacial region, which is much smaller than the entire system. In nanomaterials, however, new properties can be attained by combining several materials in the same nanosystem, where, due to the small size, the effect of synergetic properties of the separate components may become a dominant factor.[4–6] For example, Kong *et al*. prepared size-controlled Au@Cu_2O octahedral structures that exhibited excellent photocatalytic activity toward organic degradation.[7] Therefore, understanding and manipulating the semiconductor/metal interfacial structures is not only critical to enhance the desired properties of the composite materials, but also offers a new opportunity for discovering multifunctional materials with potentially exciting and unique properties.

Cu_2O as a p-type semiconductor with a direct band gap of 2.17 eV, is a material with prospective applications in photocatalysis,[7,8] solar energy conversion,[9] gas sensors,[10] negative electrode material for lithium-ion batteries,[11] templates,[6,12,13] antibacterial activity,[14] solar-driven water splitting,[15] and metal-insulator-metal resistive switching memory.[14] In the past decade, noble metal–Cu_2O heterostructures have been attracting much attention to understand the structure–property relationships. Qin *et al*. prepared micro-sized Au cubic cages with hierarchical structures using Cu_2O cubes as the starting material and these showed great microwave absorption capability.[13] Liu *et al*. have studied the selective growth of Au nanoparticles on different facets of Cu_2O microcrystals with enhanced electrocatalytic properties, indicating that the Au nanoparticles were preferentially deposited on the {111} facets because of the different surface energy between the {111} and {100} planes of Cu_2O crystals.[5] Meanwhile, Gao *et al*. reported that with the activated and shaped tips on Au petals, secondary metal structures of silver were directionally constructed on the Au flowers to generate the subsequent Au–Ag bimetallic heterostructured flowers.[4] For Cu_2O–Au heterostructures, an interesting question is whether the Au nanoparticles could also selectively grow on the same facets but in different positions such as tips or edges. However, so far, it is still a challenge to achieve selective growth only on specific positions of the seed surface, especially only on the edges or facets, and to prepare nanoparticles with edges or facets selectively coated by other substances.[16,17] This kind of selective growth is significant to the nanoscaled adjustments (structures and properties) and the preparation of novel nanostructures.

In this work, a novel Cu_2O–Au hierarchical heterostructure is reported in which Au nanograins (AuNGs) can preferentially grow on the activated and sharpened tips and edges of Cu_2O octahedrons. Unexpectedly, after the octahedrons were completely encapsulated by AuNGs layers, an unimagined nanostructure, Au nanowhiskers (AuNWs), were homogeneously formed on the AuNGs layers. In this growth process, small Au nanoparticles (AuNPs) acted as the nucleation centres of the AuNWs and with the catalysis of the pre-formed small AuNPs, the new Au nuclei continued to grow, aligned along the growth direction of the {111} axes, to form AuNWs. In the present work, we firstly prepared octahedron shaped Cu_2O crystals without any surfactants to eliminate the influence of surfactants for the selective growth of AuNGs. The procedure used to synthesize the octahedron shaped Cu_2O crystals and Cu_2O–Au heterostructures with various mophologies were shown in Scheme 1S and

[a]*Department of Materials Engineering, College of Materials and Textile, Zhejiang Sci-Tech University, Hangzhou 310018, P. R. China*
[b]*Key Laboratory of Advanced Textile Materials and Manufacturing Technology, Zhejiang Sci-Tech University, Ministry of Education, Hangzhou 310018, P. R. China. E-mail: du@zstu.edu.cn; Tel: +86-571-86843255*
[c]*MOE Key Laboratory of Macromolecular Synthesis and Functionalization, Department of Polymer Science and Engineering, Zhejiang University, Hangzhou 310027, China*
†Electronic supplementary information (ESI) available. See DOI: 10.1039/c2dt31487h

Downloaded by Zhejiang Sci Tech University on 24 November 2012
Published on 01 August 2012 on http://pubs.rsc.org | doi:10.1039/C2DT31487H

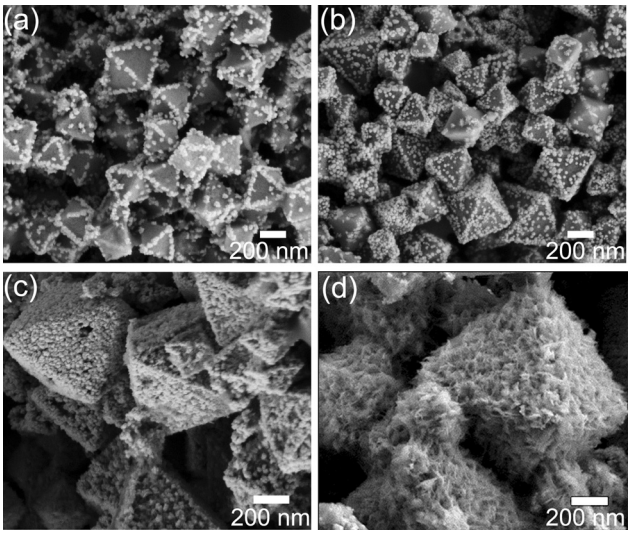

Fig. 1 (a)–(d) FE-SEM images of the AuNGs selectively grown on Cu_2O octahedron shaped crystals with different $HAuCl_4$ volumes: (a) 0.25 mL, (b) 0.50 mL, (c) 0.75 mL and (d) 1.00 mL. The concentration of the $HAuCl_4$ aqueous solution is 5 mM.

Table 1S (see ESI†). Through a galvanic reaction, $AuCl_4^-$ ions can be reduced by Cu_2O crystals directly at room temperature. With the increasing amount of $AuCl_4^-$, four novel architectures are obtained, and there are AuNGs grown along the crystal edges of Cu_2O octahedrons, AuNGs grown on the crystal facets of the Cu_2O octahedrons, Cu_2O octahedrons encapsulated by a layer of AuNGs and the AuNWs grown on AuNGs layers. Detailed experiments can be found in the ESI.†

As exemplified in Fig. 1a, it was found that most of the AuNGs with an average diameter of 27.4 ± 4.2 nm (Fig. S1, see ESI†) selectively grow on the crystal edges of the Cu_2O octahedron shaped crystals, and energy-dispersive X-ray (EDS) analysis confirms the existence of Au (Fig. 3c). From Fig. 1b, following an increasing volume of $AuCl_4^-$, not only the crystal edges are covered by AuNGs, but also the {111} facets of the Cu_2O octahedron shaped crystals. After preferentially growing on the crystal edges, numerous AuNGs are then homogeneously formed on the surface of the Cu_2O octahedrons, which is shown in Fig. 1c. With a further increase of the number of formed AuNGs, the surfaces of the Cu_2O octahedrons become rough as these AuNGs have joined together to form a solid facet, resulting in the Cu_2O octahedrons being completely encapsulated by a layer of irregular arranged AuNGs. In addition, there are some pores and splits on the AuNG layers, indicating that the AuNG layers were fabricated by etching out Cu_2O portions, which can confirm the galvanic reaction between Cu_2O and $AuCl_4^-$ (Fig. S2, see ESI†). When the volume of $AuCl_4^-$ increases to 1 mL, as seen in Fig. 1d, a large amount of AuNWs are homogeneously fabricated on the surface of AuNG layers. The AuNWs produced using this method range from 20 to 60 nm in length (Fig. S3, see ESI†).

Further studies were contemplated to understand the growth mechanism, we monitored the concentration-dependent Cu_2O–Au hierarchical heterostructures using transmission electron microscopy (TEM) and X-ray diffraction pattern (XRD) analyses. Fig. 2a–f show the TEM images of the structures

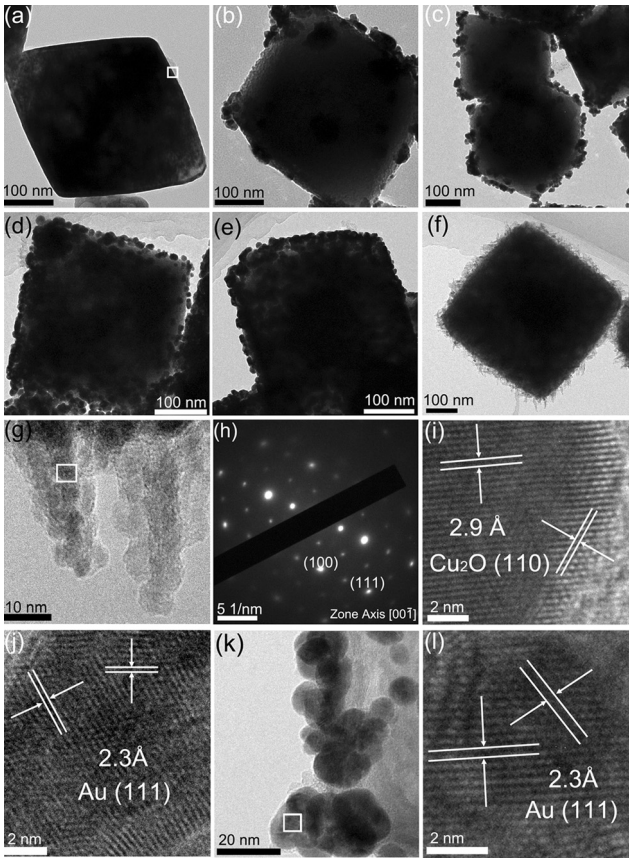

Fig. 2 TEM images of the process of the selective growth of AuNGs on Cu_2O octahedron shaped crystals with different volumes of $HAuCl_4$: (a) 0.00 mL, (b) 0.15 mL, (c) 0.25 mL, (d) 0.50 mL, (e) 0.75 mL and (f) 1.00 mL. Higher-magnification TEM image of (g) the AuNWs and (k) the AuNGs. (h) Selected area electron diffraction (SAED) pattern and (i) HRTEM image of the square region of the octahedron shaped Cu_2O crystals. HRTEM images of the square regions of (j) AuNWs and (l) AuNGs.

obtained from different volumes (0.00, 0.15, 0.25, 0.5, 0.75 and 1 mL, respectively) of $HAuCl_4$. The Cu_2O octahedrons ranging from 200 nm to 300 nm (Fig. S5, see ESI†) with smooth edges and {111} facets are shown in Fig. 2a and the SAED pattern shows the diffraction spots of Cu_2O, confirming the single crystal structure of the Cu_2O octahedron, which is shown in Fig. 2h. More TEM and FE-SEM images are shown in Fig. S4.† The HRTEM images taken near the particle edges reveal distinct lattice fringes with d spacings of 2.9 Å, which correspond to the {110} lattice planes of Cu_2O. As shown in Fig. 2b, only the tips of the octahedron are overgrown with AuNGs, and upon increasing the volume of $HAuCl_4$ to 0.25 mL, the AuNGs start to form on the crystal edges, which are shown in Fig. 2c. Fig. 2k shows the higher-magnification TEM image of the AuNGs, and these AuNGs are comprised of several small nanoparticles ranging from 5 to 10 nm in diameter. From Fig. 2d, after the AuNGs are completely arrayed along the crystal edges, the AuNGs begin to grow on the {111} facets of the octahedrons. Due to the continuous growth of AuNGs on the {111} facets, the AuNGs are packed densely on the surface of the Cu_2O octahedrons until they completely cover the octahedrons, which can be seen in

 This journal is © The Royal Society of Chemistry 2012

Published on 01 August 2012 on http://pubs.rsc.org | doi:10.1039/C2DT31487H
Downloaded by Zhejiang Sci Tech University on 24 November 2012

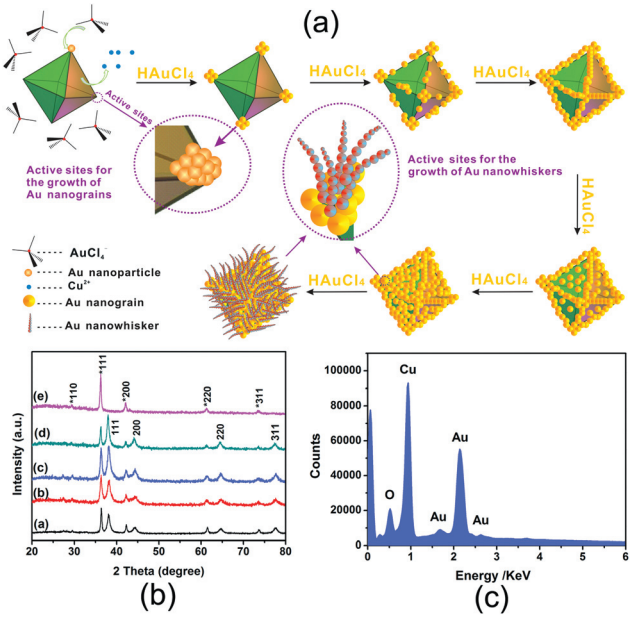

Fig. 3 (a) Schematic illustration of the selective growth process of the AuNGs on Cu_2O octahedrons. (b) XRD patterns of the intermediate products obtained at different concentrations of Au^{3+} ions during the transformation process of the octahedron Cu_2O crystals to the Cu_2O–Au hierarchical heterostructures. The volumes of $HAuCl_4$ (5 mM) are (a) 0.25 mL, (b) 0.5 mL, (c) 0.75 mL, (d) 1 mL, and (e) 0.00 mL, respectively. (c) EDS spectrum of the AuNGs grown on the edges of Cu_2O octahedrons (0.25 mL $HAuCl_4$).

Fig. 2e. When the volume of $HAuCl_4$ is further increased to 1 mL, a large amount of vimineous AuNWs are uniformly formed on the AuNGs layers with lengths ranging from 30 to 60 nm. Fig. 2g shows that small AuNPs accumulated along the growth direction to form the AuNWs. In addition, the HRTEM images (Fig. 2j and 2l) of the square regions of the AuNWs and AuNGs show fringe spacings of 2.3 Å that correspond to interplanar separation between the {111} planes, indicating that the growth direction of the AuNWs was along the {111} axes.

The present selective growth process is schematically illustrated in Fig. 3a. The driving force for the *in situ* reduction of $AuCl_4^-$ on the Cu_2O octahedrons is ascribed to the standard reduction potential difference between $AuCl_4^-$/Au (0.99 V *vs.* standard hydrogen electrode (SHE)) and Cu^-/Cu_2O (0.203 V *vs.* SHE) pairs; that is, $AuCl_4^-$ injected into the Cu_2O colloid solution can be immediately reduced by Cu_2O at room temperature.[3,4,12] The different positions of the facets of the Cu_2O octahedrons possess different surface energy, and the surface energy distribution of the octahedrons generally follows the order of $\gamma_{(facets)} < \gamma_{(edges)} < \gamma_{(tips)}$.[17–20] Therefore, the diversity of the surface energy of the same facets of the Cu_2O crystals at different positions, such as tips and edges, would lead to the preferential growth of the metal nanoparticles. As illustrated in Fig. 3a, the $AuCl_4^-$ ions were preferentially adsorbed on the tips (active sites) of the octahedrons because of their highest surface energy, and then they formed Au nuclei through a galvanic reaction.[16–18,21] More and more AuNPs formed and developed into AuNGs directly in order to reduce the surface energy of the octahedrons. These AuNGs were formed by small Au nanoparticles through coalescence and continuous growth in some regions on the surface of the octahedrons.

After the preferential growth on the tips, the AuNGs continued to grow along the edges (these possess the next-highest surface energy) of the octahedrons and further reduced the surface energy. When the surface energy of the tips and edges were reduced to the same level as that of the {111} facets of the octahedrons, the AuNGs were no longer grown on the tips and edges instead of the {111} facets. With further growth, the Cu_2O octahedrons were completely covered by AuNG layers. When the volume of the Au precursors was increased further, due to the porous structure of the AuNG layers, $AuCl_4^-$ ions can diffuse into the shell and react with the inner Cu_2O crystals. The previously formed small AuNPs can serve as nucleation centers in the growth of AuNWs. At the catalysis of the small AuNPs,[18,22,23] new Au nuclei grew continuously, aligned along the growth direction of the {111} axes to form AuNWs.

The identity and detailed crystal structure of the as-prepared Cu_2O–Au hierarchical heterostructures were analyzed using XRD characterization. The curve e (in Fig. 3(b)) shows the XRD pattern of Cu_2O crystals and all the diffraction peaks located at 29.55°, 36.42°, 42.30°, 61.34° and 73.53° (as shown in Fig. 3(b), labelled with *) can be indexed as the octahedron phases of the Cu_2O crystal (JCPDS:05-0677).[24,25] No other impurity peaks could be detected, confirming the formation of phase-pure Cu_2O. From Fig. 3(b) (from curve a to curve d), the XRD patterns of the obtained Cu_2O–Au hierarchical heterostructures suggest that the products consist of both Cu_2O and Au crystals. All the new emerging peaks, located at 38.19°, 44.39°, 64.58° and 81.72°, can be indexed as crystalline Au (JCPDS: 65-2870),[26,27] indicating that the AuNGs were successfully formed, that is, $AuCl_4^-$ can be spontaneously reduced onto the surfaces of Cu_2O without additional reductive agents at room temperature. With the increasing concentration of Au^{3+} ions from 0.25 mL to 1 mL (Fig. 3(b), from curve a to curve d), the intensity of the Au crystal peaks ({111}, {200}, {220}, {311}) became stronger, while the peaks of the Cu_2O signal ({*111}, {*200}, {*220}, {*311}) became weaker. This is consistent with the evolution processes of AuNGs grown on the surfaces of Cu_2O octahedrons. Meanwhile, it is speculated that the decreasing intensity of the Cu_2O crystal peaks was mainly caused by the etching of Cu_2O during the transformation process.

As previous research reported, Cu_2O has been used as a photocatalyst for hydrogen production and for the degradation of organic pollutants under visible light irradiation.[5,7,13] We investigated the photocatalytic performance of Cu_2O octahedrons and the as-prepared Cu_2O–Au hierarchical heterostructures towards the degradation of an organic reagent, methylene blue (MB) under a fluorescent lamp for 3 h. Fig. 4 shows the degradation (C/C_0) of MB at different reaction times and the final degradations and photographs of the MB solution after irradiation for 3 h using various photocatalysts. In a control experiment, when MB was exposed to the fluorescent lamp in the presence of H_2O_2, this led to *ca.* 25% degradation of MB (see Fig. S6 and S7 in the ESI† for detailed information). As expected, the presence of Cu_2O octahedrons led to obvious increases in the photodegradation of MB to *ca.* 68%, indicating that these Cu_2O octahedrons were photoactive and had the ability to facilitate the degradation of MB. With the selective growth of AuNGs on the

Published on 01 August 2012 on http://pubs.rsc.org | doi:10.1039/C2DT31487H
Downloaded by Zhejiang Sci Tech University on 24 November 2012

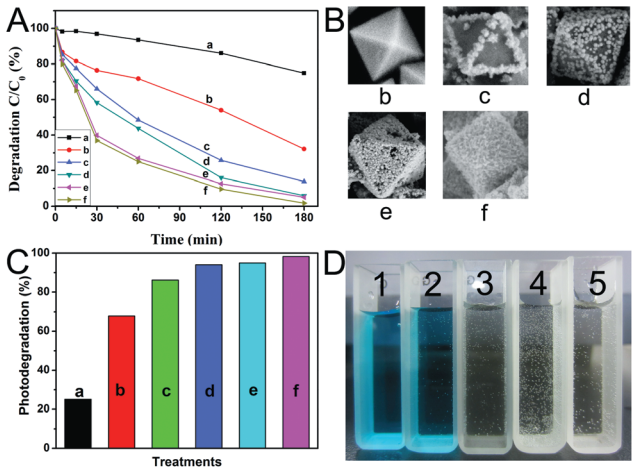

Fig. 4 (A) Degradations of MB expressed as a reduction in the intensity of absorbance of 664 nm at different irradiation times with different photocatalysts: (a) H_2O_2, (b) Cu_2O octahedrons and AuNGs grown on Cu_2O octahedrons with different volumes of $HAuCl_4$: (c) 0.25 mL, (d) 0.50 mL, (e) 0.75 mL and (f) 1.00 mL. (B) The morphologies of the corresponding photocatalysts (b–f). (C) The final percentage of photodegradation of MB as a reduction in the intensity of absorbance at 664 nm and all the samples (a–f) were under a irradiated under a fluorescent lamp (25 W, $\lambda > 400$ nm) for 3 h. (D) Photographs of the MB solution after irradiation for 3 h in the absence of H_2O_2 (1) and the presence of H_2O_2 (300 μL) (2), and in the presence of Cu_2O–Au hierarchical heterostructures (samples 3–5 are in accordance with c, e and f).

Cu_2O octahedrons, these Cu_2O–Au hierarchical heterostructures show a considerably enhanced photocatalytic activity for the degradation of MB, from *ca.* 86% to *ca.* 95%. In our metal–semiconductor systems, during the photoexcitation, electrons can migrate from the semiconductor to the metal across the Schottky barrier, where they are trapped and the electron/hole recombination phenomena are suppressed. Therefore, the hole is free to diffuse through Cu_2O to the surface where it can be used to oxidize the MB molecules. The AuNGs growth along the crystal edges of the Cu_2O octahedrons allowed *ca.* 86% degradation of MB, and with the increasing AuNGs formed on the {111} crystal facets of the Cu_2O octahedrons, the degradations improved to 94%. When the Cu_2O octahedrons were completely encapsulated by a AuNG layer, 95% degradation of MB was obtained, and the indistinctive enhanced photocatalytic activity may be partially ascribed to the relatively higher Au loading in this architecture, which might decrease the total effective Cu_2O surface area during the photocatalytic degradation of MB. Compared with the above materials' photocatalytic degradations, the AuNWs obtained the highest degradation of MB at *ca.* 98%. The AuNWs grown on the surface of AuNG layers could afford more active surface area, which can offset the negative effects of photocatalytic activity caused by higher Au loading, and this enhanced photocatalytic activity was mainly attributed to the enlarged active surface area of the AuNWs. In addition, the UV-Vis spectra of the Cu_2O octahedrons and Cu_2O–AuNWs heterostructures before and after photocatalysis were investigated, which are shown in Fig. 8S.† A weak absorption band, centered at 543 nm, was caused by the Cu_2O octahedrons (Fig. 8SA, see ESI†) and, after the photocatalysis, there is nearly no change of the Cu_2O absorption band, indicating that the surface optical properties of the material remain the same. Meanwhile, as shown in Fig. 8SB, after the growth of the AuNWs, the Cu_2O–AuNWs display obvious visible light absorption ranging from 450 to 900 nm because of the localized surface plasmon resonance of the AuNWs, presenting highly efficient light harvesting. After the photocatalysis, the absorption band centered at 545 increases to 574 nm, indicating that the noble-metal cocatalysts enhance the quantum yield of the photoinduced electron-transfer processes.[28,29]

Conclusions

In summary, we have demonstrated a novel approach for the selective growth of AuNGs on specific positions of Cu_2O octahedrons to form Cu_2O–Au hierarchical heterostructures with various Au nanostructures. FE-SEM, TEM, and XRD were used to study the morphologies, microstructures and crystal structures of these Cu_2O–Au hierarchical heterostructures, clearly indicating the selective growth process as a result of the diversity of surface energy of the facets of Cu_2O crystals at different positions such as tips and edges. In photocatalytic experiments, these Cu_2O–Au hierarchical heterostructures show fascinating degradations of MB, due to the suppressed electron/hole recombination phenomena. Due to this, the hole is free to diffuse through Cu_2O to the surface where it can be used to oxidize MB molecules. This strategy offers a new opportunity for discovering multifunctional materials with potentially exciting and unique properties.

Acknowledgements

We acknowledge the support of the project of National Natural Science Foundation of China (NSFC) (grant number: 50903072), Zhejiang Province Natural Science Foundation (grant number: Y4100197) and Science Foundation of Zhejiang Sci-Tech University (ZSTU) under number 0901803-Y.

Notes and references

1 L. Q. Mai, F. Yang, Y. L. Zhao, X. Xu, L. Xu and Y. Z. Luo, *Nat. Commun.*, 2011, **2**, 381.
2 H. G. Yang, C. H. Sun, S. Z. Qiao, J. Zou, G. Liu, S. C. Smith, H. M. Cheng and G. Q. Lu, *Nature*, 2008, **453**, 638–641.
3 C. H. Kuo, Y. C. Yang, S. J. Gwo and M. H. Huang, *J. Am. Chem. Soc.*, 2011, **133**, 1052–1057.
4 L. Gao, L. Z. Fan and J. Zhang, *Langmuir*, 2009, **25**, 11844–11848.
5 X. W. Liu, *Langmuir*, 2011, **27**, 9100–9104.
6 X. W. Liu, *RSC Adv.*, 2011, **1**, 1119–1125.
7 L. N. Kong, W. Chen, D. K. Ma, Y. Yang, S. S. Liu and S. M. Huang, *J. Mater. Chem.*, 2012, **22**, 719–724.
8 Y. H. Liang, L. Shang, T. Bian, C. Zhou, D. H. Zhang, H. J. Yu, H. T. Xu, Z. Shi, T. R. Zhang, L. Z. Wu and C. H. Tung, *CrystEngComm*, 2012, **14**, 4431–4436.
9 L. Suljo, C. Phillip and B. I. David, *Nat. Mater.*, 2011, **10**, 911–921.
10 L. L. Duan, F. Bozoglian, S. Mandal, B. Stewart, T. Privalov, A. Llobet and L. C. Sun, *Nat. Chem.*, 2012, **4**, 418–423.
11 J. Liu, S. Z. Qiao, J. S. Chen, X. W. Lou, X. R. Xing and G. Q. Lu, *Chem. Commun.*, 2011, **47**, 12578–12591.
12 F. Hong, S. D. Sun, H. J. You, S. C. Yang, J. X. Fang, S. W. Guo, Z. M. Yang, B. J. Ding and X. P. Song, *Cryst. Growth Des.*, 2011, **11**, 3694–3697.

 This journal is © The Royal Society of Chemistry 2012

13 Y. Qin, R. C. Che, C. Y. Liang, J. Zhang and Z. W. Wen, *J. Mater. Chem.*, 2011, **21**, 3960–3965.
14 S. D. Sun, X. P. Song, Y. X. Sun, D. C. Deng and Z. M. Yang, *Catal. Sci. Technol.*, 2012, **2**, 925–930.
15 S. Fukuzumi, T. Kishi, H. Kotani, Y. M. Lee and W. W. Nam, *Nat. Chem.*, 2011, **3**, 38–41.
16 N. N. Fan, Y. Yang, W. F. Wang, L. J. Zhang, W. Chen, C. Zou and S. M. Huang, *ACS Nano*, 2012, **6**, 4072–4082.
17 T. T. Tran and X. M. Lu, *J. Phys. Chem. C*, 2011, **115**, 3638–3645.
18 S. A. Dayeh, E. T. Yu and D. L. Wang, *J. Phys. Chem. C*, 2007, **111**, 13331–13336.
19 Z. C. Xu, E. Lai, S. H. Yang and H. S. Kimberly, *Chem. Commun.*, 2012, **48**, 5626–5628.
20 G. R. Zhang, D. Zhao, Y. Y. Feng, B. S. Zhang, D. S. Su, G. Liu and B. Q. Xu, *ACS Nano*, 2012, **6**, 2226–2236.
21 C. G. Read, E. M. P. Steinmiller and K. S. Choi, *J. Am. Chem. Soc.*, 2009, **131**, 12040–12041.
22 M. A. Mahmoud, W. Qian and M. A. El-Sayed, *Nano Lett.*, 2011, **11**, 3285–3289.
23 C. H. Kuo, T. E. Hua and M. H. Huang, *J. Am. Chem. Soc.*, 2009, **131**, 17871–17878.
24 P. Lignier, R. Bellabarba and R. T. P. Tooze, *Chem. Soc. Rev.*, 2012, **41**, 1708–1720.
25 W. C. Huang, L. M. Lyu, Y. Ch. Yang and M. H. Huang, *J. Am. Chem. Soc.*, 2012, **134**, 1261–1267.
26 H. Zhu, M. L. Du, M. L. Zou, C. S. Xu, N. Li and Y. Q. Fu, *J. Mater. Chem.*, 2012, **22**, 9301–9307.
27 H. Zhu, M. L. Du, M. L. Zou, C. S. Xu and Y. Q. Fu, *Dalton Trans.*, 2012, DOI: 10.1039/c2dt30998j.
28 P. V. Kamat, *J. Phys. Chem. Lett.*, 2012, **3**, 663–672.
29 M. Achermann, *J. Phys. Chem. Lett.*, 2010, **1**, 2837–2843.

Published on 01 August 2012 on http://pubs.rsc.org | doi:10.1039/C2DT31487H
Downloaded by Zhejiang Sci Tech University on 24 November 2012